

This article was downloaded by:

On: 25 January 2011

Access details: *Access Details: Free Access*

Publisher *Taylor & Francis*

Informa Ltd Registered in England and Wales Registered Number: 1072954 Registered office: Mortimer House, 37-41 Mortimer Street, London W1T 3JH, UK



Separation Science and Technology

Publication details, including instructions for authors and subscription information:

<http://www.informaworld.com/smpp/title~content=t713708471>

Effects of a Carrier and Its Diluent on the Transport of Metals across Supported Liquid Membranes (SLM). I. Solubility Mechanism

A. A. Elhassadi^a; D. D. Do^a

^a Department of Chemical Engineering, University of Queensland, St. Lucia, Queensland, Australia

To cite this Article Elhassadi, A. A. and Do, D. D. (1986) 'Effects of a Carrier and Its Diluent on the Transport of Metals across Supported Liquid Membranes (SLM). I. Solubility Mechanism', *Separation Science and Technology*, 21: 3, 267 – 283

To link to this Article: DOI: 10.1080/01496398608058377

URL: <http://dx.doi.org/10.1080/01496398608058377>

PLEASE SCROLL DOWN FOR ARTICLE

Full terms and conditions of use: <http://www.informaworld.com/terms-and-conditions-of-access.pdf>

This article may be used for research, teaching and private study purposes. Any substantial or systematic reproduction, re-distribution, re-selling, loan or sub-licensing, systematic supply or distribution in any form to anyone is expressly forbidden.

The publisher does not give any warranty express or implied or make any representation that the contents will be complete or accurate or up to date. The accuracy of any instructions, formulae and drug doses should be independently verified with primary sources. The publisher shall not be liable for any loss, actions, claims, proceedings, demand or costs or damages whatsoever or howsoever caused arising directly or indirectly in connection with or arising out of the use of this material.

Effects of a Carrier and Its Diluent on the Transport of Metals across Supported Liquid Membranes (SLM). I. Solubility Mechanism

A. A. ELHASSADI and D. D. DO

DEPARTMENT OF CHEMICAL ENGINEERING
UNIVERSITY OF QUEENSLAND
ST. LUCIA, QUEENSLAND 4067, AUSTRALIA

Abstract

A new phenomenon called the solubility mechanism was observed experimentally and explained theoretically. This phenomenon helps to explain the nonmonotonic behavior of the flux with respect to the carrier concentration through the use of a simplified model. The reason why the linear behavior of the flux-carrier relationship was observed by past theories is because they ignore a process which occurs simultaneously with the carrier-metal reaction. We believe that this process is the solubility process in which the metal distribution within the organic phase is a function of both carrier and diluent concentrations.

INTRODUCTION

When studying the transport across liquid membranes impregnated with a carrier and a diluent, one generally tends to believe that the flux increases linearly with increasing carrier concentration according to Fick's first law of diffusion. Lee et al. (6) developed a theoretical model where the flux is proportional to the carrier concentration even though their experimental finding showed that the flux approaches a limiting value as the carrier concentration is increased. Danesi et al. (4) were able to explain this limiting flux behavior by incorporating diffusional resistance through the membrane, interfacial reaction resistance, and aqueous diffusional resistance within the aqueous boundary layer. However, they concluded that the flux relationship with carrier con-

centration remains limiting at a slope of zero rather than going through a maximum.

Babcock et al. (1, 2) found experimentally that in coupled transport of uranium with Alamine 336, the flux increases with carrier concentration, reaching a maximum value at about 30 vol% carrier concentration, above which the flux decreases with increasing carrier concentration. This interesting phenomenon was believed to be caused by two competing factors: the concentration gradient of the uranium complex and the viscosity of the organic phase in the liquid membrane. Babcock et al. (1, 2) failed to explain the phenomenon quantitatively but pointed out the dominant effects that cause this phenomenon to be:

- (1) Carrier concentration effects
- (2) Pore size effects
- (3) Interfacial effects

Baker et al. (3) observed a similar phenomenon of limiting flux with respect to the metal concentration in the feed solution. This phenomenon was termed "saturation phenomena" where the limiting effect was due to saturation of the organic phase with the metal-carrier complex. They concluded that the saturation phenomenon was caused mainly by the solubility and not the stoichiometry of the system. This conclusion was supported indirectly by the observation of a green, water-insoluble, organic-soluble precipitate formed at the feed-membrane interface. It is worth mentioning here that a similar observation was observed in this study. When the carrier is diluted with more diluent, the limiting factor becomes the stoichiometry where the supply of available carrier rather than the solubility is important.

This paper will aim at explaining the behavior of the flux with respect to the whole range of carrier concentration. It has been found experimentally (1-4, 6) that there is a flux at 0% carrier concentration (i.e., 100% diluent). This interesting experimental finding was left unexplained, and theoretically the flux was assumed to be zero at 0% carrier concentration. We propose here that because of nonzero permeability (or flux) at 0% carrier concentration, the metal transported through the membrane must be by passive diffusion (7). This is at least applicable when the metal concentration at the feed solution is much greater than the metal concentration at the strip solution.

THEORY

Consider a membrane matrix impregnated with a mixture of a carrier

and a diluent. Here, we propose a mechanism for the transport of metal through a supported liquid membrane. The following steps are necessary:

- (1) Distribution of the metal from the aqueous phase to the liquid membrane phase (i.e., the diluent, the carrier, or their mixture).
- (2) Either (a) passive diffusion of the metal through the diluent or (b) the metal combines with the carrier and the resulting complex diffuses across the membrane.
- (3) At the other side of the membrane, the energy-supplying ion reacts with the carrier complex, releasing the metal.
- (4) Return of the carrier and diluent across the membrane. This mechanism is schematically illustrated in Fig. 1. It is different from the classical accepted mechanism (5) which assumes the distribution of the carrier from organic into aqueous phase. The classical description cannot be accepted because it violates the integrity of the impregnated membrane.

We believe that the following effects are essential to the development of a comprehensive theory that explains the experimental results quite closely. These effects are: 1) effects of carrier and diluent, 2) pore size effects, and 3) interfacial effects. In this simplified model development, we only look at diffusional aspects of the carrier and diluent in the membrane. The viscosity and pore size effects are lumped in the diffusion coefficient. The interfacial effects can be eliminated through stirring above the standard rate to overcome concentration polarization, and the interfacial reaction rate is assumed to be faster than the diffusion rate so that an equilibrium relationship can be invoked.

We denote the concentrations of the metals in the aqueous and liquid membrane phases as M and M^* , respectively. The distributed metal concentration in the liquid membrane phase could be written as

$$M^* = M[\alpha x + \beta(1 - x)] \quad (1)$$

where α is the distribution coefficient when the carrier concentration is 100% and β is the distribution coefficient when the diluent concentration is 100%. It must be emphasized at this point that α and β are not intrinsic constants but rather they are functions of various parameters such as acid concentrations, ligand concentrations, loading of the metal, and structure of the membrane (1-7).

We will assume that the organic phase chemical reaction is very fast relative to diffusion so that equilibrium can be achieved at all times. The stoichiometry relation is

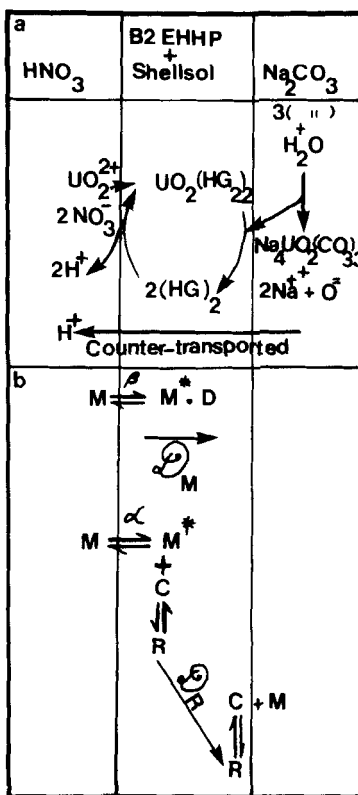


FIG. 1. Postulated mechanism. (a) Uranium transport from the feed phase (HNO_3) to the strip phase (Na_2CO_3) through a B2EHHP-supported liquid membrane. (b) Distribution of metal into the diluent (D) and carrier (C) phases.

$$\text{M}^*|_o + \text{C}|_o \rightleftharpoons \text{R}|_o \quad (2)$$

where C represents the number of carrier molecules needed to complex the metal and R represents the metal-carrier complex. The subscript o denotes the organic phase. The metal carrier concentration could be expressed as

$$R = K_E C M^* \quad (3)$$

If we denote x as the initial concentration of the carrier, the following mass balance equation must hold at all times:

$$x = C + R \quad (4)$$

Combining Eqs. (1), (3), and (4) yields the following relationship between the free carrier concentration and the metal–carrier complex concentration

$$C = \frac{R}{K_E M [\alpha x + \beta(1 - x)]} \quad (5)$$

Substitution of Eq. (5) into Eq. (4) gives R to be

$$R = \frac{K_E M [\alpha x + \beta(1 - x)] x}{1 + K_E M [\alpha x + \beta(1 - x)]} \quad (6)$$

Two special cases of Eq. (6) are worth mentioning. For very low metal concentrations (i.e., $K_E M [\alpha x + \beta(1 - x)] \ll 1$), Eq. (6) could be written as

$$R = K_E M [\alpha x + \beta(1 - x)] x \quad (6a)$$

For very high metal concentrations (i.e., $K_E M [\alpha x + \beta(1 - x)] \gg 1$), Eq. (6) could be written as

$$R = x \quad (6b)$$

Now we can write Fick's first law of diffusion for the system illustrated in Fig. 1 as

$$J = \frac{D_R}{\delta} [(R)_o - (R)_\delta] + \frac{D_M^*}{\delta} [(M^*)_o - (M^*)_\delta] \quad (7)$$

where δ denotes the other side of the membrane.

The analysis can be simplified by further assuming:

- (a) $(R)_o \gg (R)_\delta$
- (b) The second term in the right-hand side is negligible
- (c) Steady state
- (d) Very low metal concentrations
- (e) Linear concentration gradients through the membrane

With these simplifying assumptions and with substitution of Eqs. (1), (3), and (6), Eq. (7) becomes

$$J = \frac{D_R}{\delta} K_E M x [\alpha x + \beta(1 - x)] \quad (8)$$

Finally, to calculate α , β , and x_{\max} , we need to look at the functional behavior of flux with respect to the volume fraction of carrier, x . We can write this function from Eq. (8) as

$$f(x) = x[\alpha x + \beta(1 - x)] \quad (8a)$$

This function possesses a maximum at

$$x_{\max} = \frac{1}{2} \left[1 - \frac{\alpha}{\beta} \right]^{-1} \quad (9)$$

In order for the theory to be applicable at this simplified level, x_{\max} must be greater than 50%. Equation (9) also tells us that the maximum flux or permeability will occur at a positive maximum volume fraction when

$$\alpha/\beta < 1 \quad (10)$$

This is a very interesting finding because it justifies the proposed mechanism and gives explanation to the accepted limiting effect of the solubility (3) which is due to saturation of the organic phase. Equation (10) simply says that the function of the diluent is to attract and dissolve the metal in the organic phase more than the carrier does. This is verified by the findings of Babcock (1, 2) which roughly state: "With increasing concentration of the carrier in the diluent both the amount of metal that can be extracted into the membrane and the viscosity of the organic solution increase. However, these opposing effects are the cause behind the maximum."

From Eq. (8), one can evaluate the flux at $x = 1$ (i.e., pure carrier)

$$J_{x=1} = \frac{D_R K_E}{\delta} (M) \alpha \quad (11)$$

Dividing Eqs. (8) by (11) yields

$$\frac{J}{J_{x=1}} = x \left[x + \frac{\beta}{\alpha} (1 - x) \right] \quad (12)$$

To get the optimal ratio β/α that give us the best fit, we need to use the

simple linear regression analysis technique. The least square criterion is used to minimize the sum of the squares of the vertical distances between the experimental points and the theoretical estimations. The value β/α which minimizes this sum is the desired value. This could be interpreted mathematically as follows:

$$\sum_{i=1}^n \left\{ \left(\frac{J}{J_{x=1}} \right)_{\text{exp}} - \left. \frac{J}{J_{x=1}} \left(x, \frac{\beta}{\alpha} \right) \right|_{\text{model}} \right\} = 0 \quad (13)$$

where n is the number of data points used. Substitution of Eq. (12) into (13) gives

$$\sum_{i=1}^n \left\{ \left(\frac{J}{J_{x=1}} \right)_{\text{exp}} - x \left[x + \frac{\beta}{\alpha} (1 - x) \right] \right\} = 0 \quad (14)$$

Therefore, to calculate the flux at any point x , we need to measure

- The optimal value β/α which satisfies Eq. (14) for all data points available
- Using Eq. (12), calculate other fluxes J_k
- Finally, compare the theoretical fluxes with the measured ones

EXPERIMENTAL

A. Reagents and Membranes

The carrier used was Bis (2-ethylhexyl) hydrogen phosphate (denoted by B2EHHP) which was manufactured by Aldrich Chemical, Inc. This agent has the formula $[\text{CH}_3(\text{CH}_2)_3\text{CH}(\text{C}_2\text{H}_5)-\text{CH}_2\text{O}]_2\text{P}(\text{O})\text{OH}$ (98%) with an approximate structure depicted schematically in Fig. 2. The diluent used was Shellsol 2046 manufactured by Shell Chemicals, Inc. Shellsol 2046 is a high boiling, high flash point hydrocarbon solvent.

All aqueous solutions were prepared from reagent grade chemicals. The source solution was uranyl nitrate dissolved in nitric acid. The sink solution was sodium carbonate.

The hydrophobic organic phase forming the liquid membrane was immobilized within the pores of Celgard 2500, a microporous polypropylene film from Celanese Plastics Co. This membrane is approximately 25 μm thick, has a nominal porosity of 45%, with a pore diameter

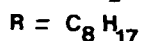
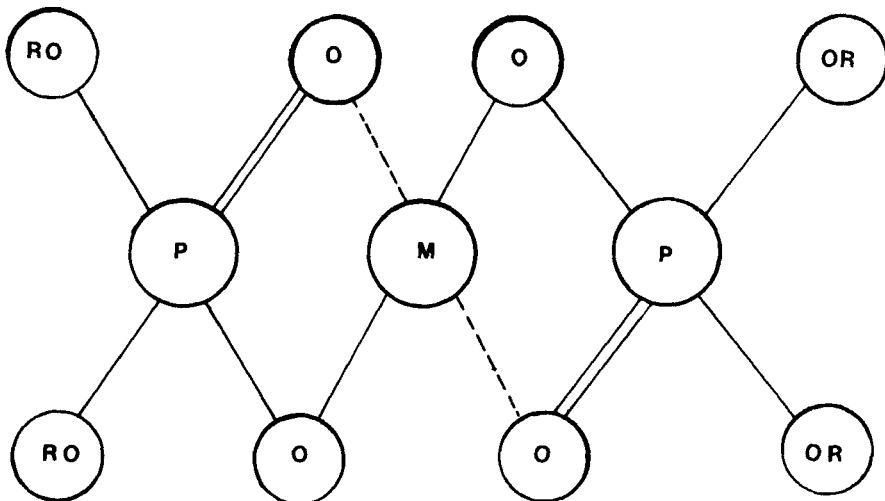


FIG. 2. The structure of the carrier agent.

of the order of 0.01 μm . Some pictures of the membrane are showing in Fig. 3. Filling the pores of these membranes with the carrier and diluent was accomplished by immersing the membrane within the organic solution with moderate vacuum applied.

B. Permeability Measurements

A picture of the apparatus is shown in Fig. 4. It consists of two glass vessels, each one having a volume of 500 mL. The two vessels are clamped together through two flanges facing each other, giving a cross-sectional area of 25 cm^2 where the membrane is positioned. The membrane is protected by two Teflon gaskets. The two chambers were stirred continuously by stainless steel stirrers driven by electric motors. Each cell was provided with a sampling port, a stirrer port, and a pH-electrode port. The pH and metal ion concentrations of the solutions on

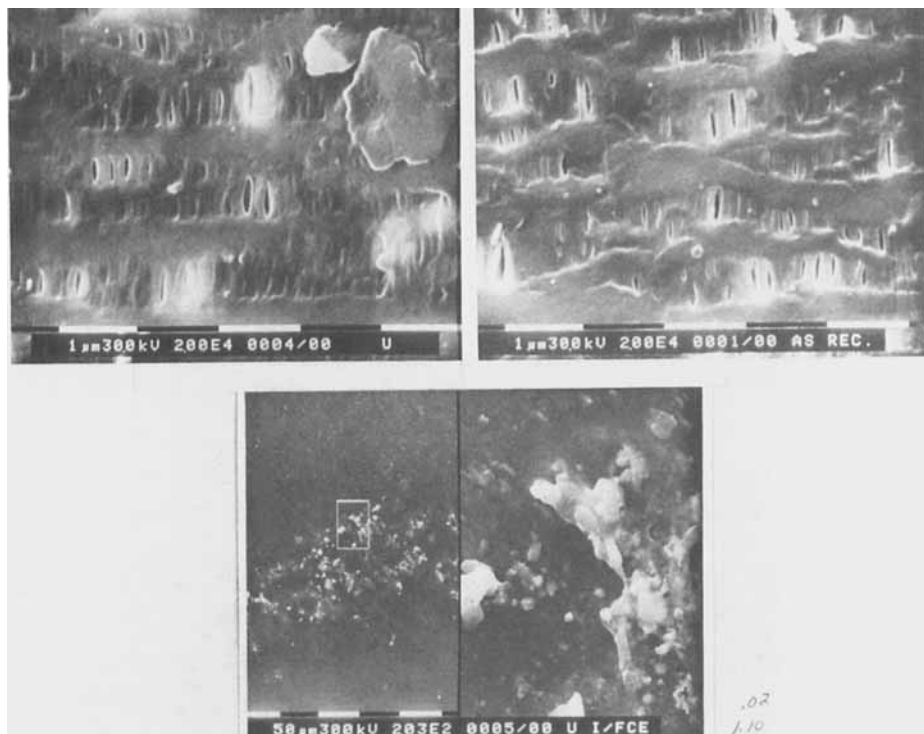


FIG. 3. Photomicrograph of untreated and treated Celgard 2500 film.

each side were measured by removing known volumes with a pipette for analysis. The permeability was obtained from the concentration vs time data after correction for sampling. All permeation experiments were carried out at room temperature.

RESULTS AND DISCUSSION

Figure 5 shows the passive transport of uranium through the B2EHHP supported liquid membrane. As shown, uranium only flows in one direction, from the feed side to the strip side. With a carrier concentration of 50%, a feed solution of 0.013 M uranium in HNO_3 ($\text{pH} = 0.70$), and a 1 M Na_2CO_3 strip solution which contained no uranium, the uranium was transported as illustrated in Fig. 5. Figure 6 shows the behavior of pH vs



FIG. 4. Experimental apparatus for measuring the permeability.

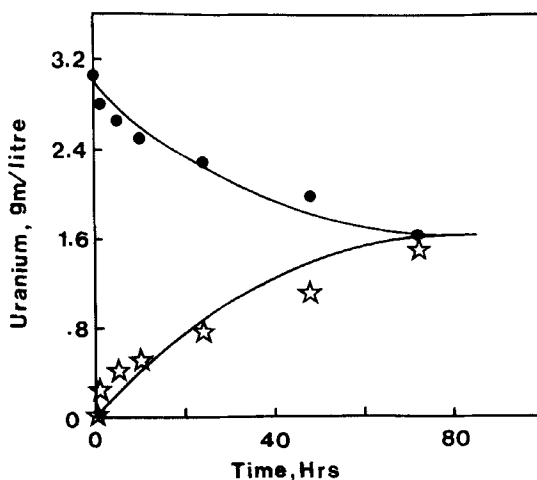


FIG. 5. Passive transport of uranium through a B2EHHP (50%) supported liquid membrane vs time. (●) Feed side (0.13 M U, HNO_3 ($\text{pH} = 0.70$)). (★) Strip side (1 M Na_2CO_3 ($\text{pH} = 12.5$))).

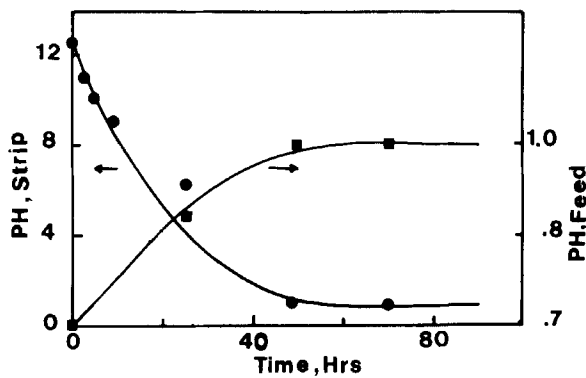


FIG. 6. pH behavior of feed and strip sides with time. (■) Feed side (0.01 M U, HNO_3 ($\text{pH} = 0.70$))). (○) Strip side (1 M Na_2CO_3 ($\text{pH} = 12.5$))). 100% Shellsol.

time for the feed and source sides with conditions illustrated in the figure. Figures 7 and 8 were used to evaluate the permeability coefficients from the slopes of the straight lines obtained by plotting $\ln(C/C_0)$ vs time (s). The slopes of the straight lines are equal to $-(A\varepsilon/V)P$, where A (membrane area) = 25 cm², ε (Celgard 2500 membrane porosity) = 0.45, and V (volume of aqueous feed solution) = 500 cm³.

A. Effect of Carrier Concentration

Figures 9 and 10 show the complex behavior of the uranium flux vs B2EHHP concentration in the supported liquid membrane. With increasing carrier concentration, the flux increases, reaching a maximum value at about 51 and 70% carrier concentration in Figs. 9 and 10, respectively. This behavior of the flux-carrier concentration relationship is different from what is expected from Fick's first law of diffusion. Figures 9 and 10 also show the theoretical predictions of the flux by the simple theory presented in this paper. Babcock et al. (2) reported calculated flux values using Fick's law and the Stokes-Einstein equation as much as five times larger than the experimental flux values. It is clear from Figs. 9 and 10 that the calculated fluxes agree very well both

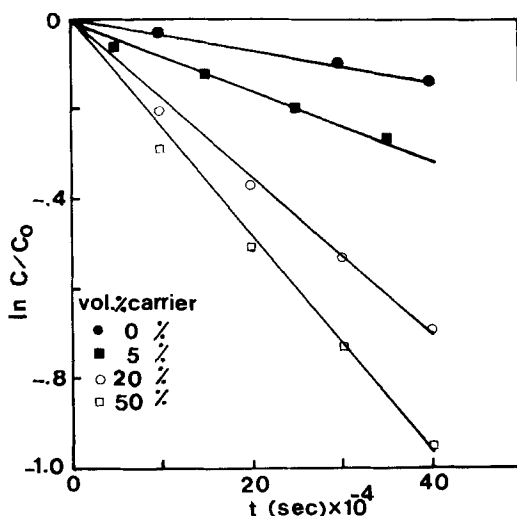


FIG. 7. Membrane permeation data of U metal. Feed side: 0.01 M U, HNO₃ (pH = 1.5). Strip side: 1 M Na₂CO₃ (pH = 12.5).

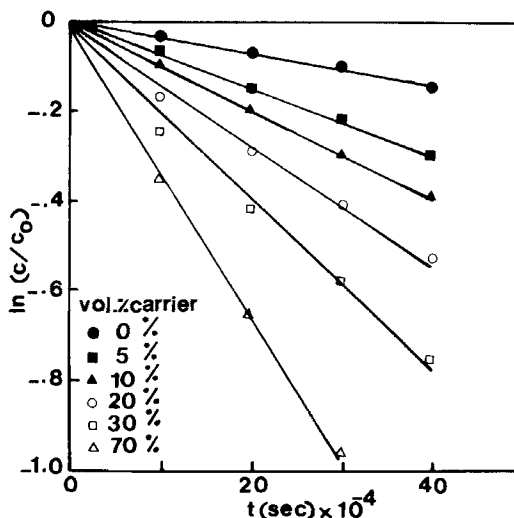


FIG. 8. Membrane permeation data of U metal Feed side: 0.013 M U, HNO₃ (pH = 1). Strip side: 1 M Na₂CO₃ (pH = 12.5).

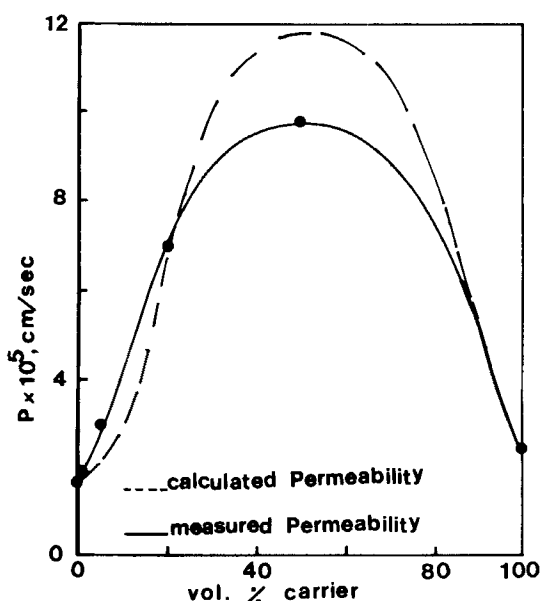


FIG. 9. Uranium permeability as a function of carrier concentration. Permeability coefficient values are related to permeation data in Fig. 7.

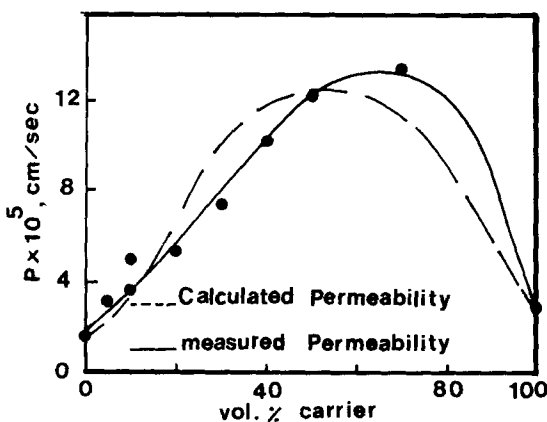


FIG. 10. Uranium permeability as a function of carrier concentration. Permeability coefficient values are related to permeation data in Fig. 8.

qualitatively and quantitatively with the measured flux values. The x_{\max} of 0.50 and 0.50 are compared to 0.51 and 0.70 values obtained experimentally in Figs. 9 and 10, respectively. The experimental results indicate that the theoretical findings represent an approximate but nevertheless useful prediction of the behavior of flux.

B. Pore Size and Viscosity Effects

Babcock et al. (2) attributed the cause of this "maximal phenomenon" to be the concentration gradient of the uranium complex, the viscosity of the organic phase and hindered diffusion of the uranium complex caused by aggregation of the complex, and the tortuosity of the pores of the membrane. So far, the effect of all these important parameters has been lumped in the diffusion coefficient of our model. This is the main reason why the model predicts only the behavior of the flux for maximums that occur at greater than 50% of carrier concentration. Babcock et al. (2) obtained a maximum at 30 vol% Alamine 336. Also, it has been assumed that all the carrier is being complexed by the available metal distributed to the carrier phase.

Baker et al. (3) did not observe the maximum phenomenon with their copper-Lix64N system using three different diluents (kerosene, mineral oil, and dop). The reason is that this complex phenomenon might be a function of the carrier, the diluent, the metal, and loading of the metal to

the organic phase. However, it is believed that this maximal phenomenon might occur not only with carrier concentration but with pH (1, 2), acid concentration (7), ligand concentration (7), and metal concentration (7).

Interfacial effects were not accounted for by simply assuming fast interfacial chemical reactions and by stirring at about 1000 rpm which is sufficient to eliminate any concentration polarization. At this high stirring rate we made sure that the integrity of the liquid membrane was conserved.

C. Morphology of the Microporous Membranes

As seen from Fig. 3, the micropores consist of elongated slits, arranged in rows. Both sides of each specimen were examined, and their appearances are similar. The sizes and distribution of the pores change considerably over the surface of the membrane. An accumulation of solid material could be seen with the naked eye in the case of treated membrane samples with uranium. The data printout on each picture is explained as follows:

1 μm = length of each white scale

3.00 kV = gun potential

2.00 E4 = magnification

0.001 = picture #

00 = code #

As Rec = As received

U = treated with uranium

UI/FCE = uranium interface

CONCLUSIONS

Transport phenomenon within supported liquid membrane is a complex process limited by hindered diffusion, composition of the organic phase, and interfacial effects. Even though the process is complex, we were able with the use of a simplified model to predict closely the permeability (or the flux) behavior with respect to carrier concentration. We have also demonstrated that the maximal behavior that occurs with carrier concentration could occur with the rest of the variables controlling the system. The theory is so simple that we need only to specify the maximum point and determine the flux or the

permeability at 100% carrier concentration in order to predict the flux or the permeability at any other point.

SYMBOLS

A	membrane area
B2EHHP	bis(2-ethylhexyl) hydrogen phosphate
C	carrier concentration at time t
D_R	diffusivity of the metal-carrier complex
D_M	diffusivity of the metal in the organic phase
$f(x)$	functional behavior of the flux
J	solute flux
K_E	equilibrium constant for the metal-carrier complex formation reaction
M	concentration of the metal in the aqueous phase
M^*	concentration of the metal in the organic phase
P	membrane permeability
R	metal-carrier concentration
U	uranium concentration
V	volume of aqueous feed solution
x	initial concentration of the carrier in the diluent
x_{\max}	concentration where flux is maximum

Greek Letters

α	the distribution coefficient in a pure carrier
β	the distribution coefficient in a pure diluent
δ	thickness of the membrane
ϵ	porosity of the membrane

Subscripts

a	aqueous phase
o	organic phase
0	zero thickness of the membrane
δ	δ thickness of the membrane

Acknowledgments

The authors wish to acknowledge Mr Bell Free of Hardie Trading Company and Dr G. J. Sheehan of MIM for their supply of Celgard 2500 microporous membranes and Shellsol 2046, respectively. The authors also wish to thank Mr J. V. Hardy for his electron microscopic photographs.

REFERENCES

1. W. C. Babcock, R. W. Baker, E. D. La Chapelle, and K. L. Smith, "Coupled Transport Membranes II: The Mechanism of Uranium Transport with a Tertiary Amine," *J. Membr. Sci.*, 7, 71 (1980).
2. W. C. Babcock, R. W. Baker, E. D. La Chapelle, and K. L. Smith, "Coupled Transport Membranes III: The Rate-Limiting Step in Uranium Transport with a Tertiary Amine," *Ibid.*, 7, 89 (1980).
3. R. W. Baker, M. E. Tuttle, D. J. Kelly, and H. K. Lonsdale, "Coupled Transport Membranes I: Copper Separations," *Ibid.*, 2, 213 (1977).
4. P. R. Danesi, E. P. Horwitz, G. F. Vandegrift, and R. Chiarizia, "Mass Transfer Rate through Liquid Membranes: Interfacial Chemical Reactions and Diffusion as Simultaneous Permeability Controlling Factors," *Sep. Sci. Technol.*, 16(2), 201 (1981).
5. I. Komasawa, T. Otake, and A. Yamada, "Equilibrium Studies of Copper Extraction from Sulphate Media with Hydroxyomie Extractant," *J. Chem. Eng. Jpn.*, 13(2), 130 (1980).
6. K. Lee, D. F. Evans, and E. L. Cussler, "Selective Copper Recovery with Two Types of Liquid Membranes," *AIChE J.*, 24(5), 860 (1978).
7. H. Matsuoka, M. Aizawa, and S. Suzuki, "Uphill Transport of Uranium across a Liquid Membrane," *J. Membr. Sci.*, 7, 11 (1980).

Received by editor April 30, 1985